Phylogenomics, biogeography, and trait evolution of the Boletaceae (Boletales, Agaricomycetes, Basidiomycota)

Keaton Tremble[a]*, Terry Henkel[b], Alexander Bradshaw[a], Colin Domnauer[a], Lyda Brown[a], Lê Xuân Thám[c], Guliana Furci[d], Cathie Aime[e], Jean-Marc Moncalvo[f], Bryn Dentinger[a]*

[a]Natural History Museum of Utah and School of Biological Sciences, University of Utah, Salt Lake City, Utah 84108

[b]Department of Biological Sciences, California State Polytechnic University, Humboldt, Arcata, California 95521

[c]Van Lang University, Ho Chi Minh City, Viet Nam

[d]Fungi Foundation, Brooklyn, New York 11222

[e]Department of Botany and Plant Pathology, Purdue University, West Lafayette, Indiana 47907

[f]Department of Natural History, Royal Ontario Museum & Department of Ecology and Evolutionary Biology, University of Toronto, Toronto M5S 2C6, Canada

ABSTRACT

The species-rich porcini mushroom family Boletaceae is a widespread and well-known group of ectomycorrhizal (ECM) mushroom-forming fungi that has eluded intrafamilial phylogenetic resolution despite many attempts using morphological traits and multi-locus molecular datasets. In this study, we present a genome-wide molecular dataset of 1764 single-copy gene families from a global sampling of 418 Boletaceae specimens. The resulting phylogenetic analysis has strong statistical support for most branches of the tree, including the first statistically robust backbone. The enigmatic *Phylloboletellus chloephorus* from non-ECM Argentinian subtropical forests was recovered as an early diverging lineage within the Boletaceae. Time-calibrated branch lengths estimate that

the family first arose in the early- to mid-Cretaceous and underwent a rapid radiation in the Eocene, possibly when the ECM nutritional mode arose with the emergence and diversification of ECM angiosperms. Biogeographic reconstructions reveal a complex history of vicariance and episodic long-distance dispersal correlated with historical geologic events, including Gondwanan origins and cladogenesis patterns that parallel its fragmentation. Ancestral state reconstruction of sporocarp morphological traits predicts that the ancestor of the Boletaceae was lamellate with ornamented basidiospores, contrary to most contemporary "bolete" morphologies. Transition rates indicated that the lamellate hymenophore and sequestrate sporocarp are reversible traits. Together, this study represents the most comprehensively sampled, data-rich molecular phylogeny of the Boletaceae to date, enabling robust inferences of trait evolution and biogeography in the group.

KEYWORDS: phylogenomics; Boletaceae; porcini; evolutionary radiation; Gondwana

INTRODUCTION

Evolutionary radiations result from short bursts of relatively rapid diversification and demonstrate the creative power of evolution. Adaptive and non-adaptive radiations may be the most common macroevolutionary patterns and are fundamental to the origins of biodiversity (Simoes et al. 2016; Futuyma 1998; Schluter and McPeek 2000). Yet, the causes of evolutionary radiations are poorly known for most groups, as most studies have focused on animals and plants (Soulebeau et al. 2015). The other major multicellular eukaryotic group, the Fungi, have largely been neglected (Varga et al. 2019).

The porcini mushroom family Boletaceae (FIG. 1) is an example of an evolutionary radiation in Fungi (Bruns et al. 1992). The family is exceptionally diverse (>2000 currently accepted species) and globally distributed, but poorly documented for

many regions. Yet, boletoid fungi are prevalent ectomycorrhizal (ECM) mutualists in ecosystems dominated by ECM plants (Peay et al. 2010) and at least eight species are traded globally as wild-collected edible mushrooms (Arora 2008; Sitta and Floriani 2008; Dentinger et al. 2010; Dentinger and Suz 2014). Despite their conspicuous sporocarps, ecological dominance, and cultural importance, new species of Boletaceae are regularly described from poorly explored habitats around the globe (e.g. Halling et al. 2006, 2023; Fulgenzi et al. 2007, 2008, 2010; Neves et al. 2010; Husbands et al. 2013; Castellano et al. 2016; Chakraborty et al. 2015; Das et al. 2015, 2016; Henkel et al. 2016; Magnago et al. 2017). New species have also recently been described from wild-collected foods in markets (e.g. Das et al. 2015; Dentinger and Suz 2014; Halling et al. 2014). While new Boletaceae species are increasingly understood in a global phylogenetic context, shedding light on their origin, diversification, and migration, over 20 years of molecular phylogenetic studies using legacy loci have made little progress towards resolving the deepest nodes ("backbones") in Boletaceae phylogenies (Grubisha et al. 2001; Binder and Hibbett 2006; Drehmel et al. 2008; Dentinger et al. 2010; Nuhn et al. 2016; Wu et al. 2014).

A prominent consequence of this lack of phylogenetic resolution is the recent explosion of new generic names to accommodate newly discovered species, or species that are included in molecular phylogenetic analyses for the first time and recovered on long branches with no supported affinity to existing named genera (e.g., Castellano et al. 2016; Henkel et al. 2016; Badou et al. 2022; Halling et al. 2023). Few of these studies have followed recommended best practices for naming new genera (Vellinga et al. 2015). Moreover, many of these new Boletaceae genera are monotypic and require identification to recognize, an impractical solution to the problem. Taken together, the

current situation is perhaps best described as a quagmire of nomenclatural, taxonomic, ecological, and evolutionary speculation.

Beyond taxonomic concerns, the Boletacaeae presents a unique system to identify the genetic mechanisms that contribute to diversification. The Boletaceae appear to have underwent an early evolutionary radiation between 60-100 mya (Bruns and Palmer 1989; Binder et al. 2006; Dentinger et al. 2010; Wu et al. 2014, 2016; Sato et al. 2019). This early radiation has been correlated with the convergent evolution of morphological traits, such as the lamellate hymenophore and gasteromycetization (Castellano et al. 2016), suggesting that emergence of morphological diversity is constrained by relatively few changes in developmental pathways.

Many factors have contributed to difficulties in generating robust phylogenetic reconstructions for the Boletaceae. While phenomena such as incomplete lineage sorting and hybridization may obscure historical phylogenetic signal, previous datasets for the Boletaceae had patchy taxonomic and geographic sampling. These factors impact accurate phylogenetic reconstruction, possibly exacerbated by the aforementioned rapid radiation event (Bruns et al. 1992; Sato et al. 2017). Without a phylogeny that is based on globally representative taxon sampling and statistically well-supported resolution at all depths of the tree, it is impossible to name, classify, and understand evolutionary history in the Boletaceae. For example, only a few recent studies have included representatives of the exceptionally rich Australian boletoid funga (Halling, Fechner, et al. 2015, 2023; Halling, Nuhn, et al. 2012). Boletoid fungi from the Neotropics and Afrotropics are rarely represented in family-level analyses despite their exceptional species richness (e.g. Heinemann 1951; Henkel et al. 2012).

Recent fieldwork has resulted in many new collections from under-sampled regions (B. Dentinger, T. Henkel, R. Halling; unpublished data), and these are now

available to include in phylogenetic datasets aiming to achieve the first globally representative sampling of the Boletaceae. Collections-based phylogenomics is also effective for resolving ancient relationships among mushroom-forming fungi (Dentinger et al. 2015; Liimatainen et al. 2021; Tremble et al. 2020). However, no one has yet applied these methods to the Boletaceae. Moreover, whole genome sequencing of mushroom forming fungi provides opportunities to go beyond phylogenetic reconstruction. For example, whole genome sequencing can exceed legacy loci in identifying population processes that generate biodiversity (e.g. Tremble et al. 2022).

For this study, we generated the first phylogeny of the Boletaceae that utilized a very large molecular dataset comprised of 1764 genome-wide loci from 418 taxa across the family. Specimens were collected in many tropical and temperate geographic regions. To obtain broad geographic and taxon coverage we included type fungarium specimens and recent new collections. We utilized specimens from previously under-sampled regions including tropical Africa, southern South America, lowland tropical South America, and Australia. Type species were sampled to facilitate future taxonomic revisions of genera. Using our highly resolved genome-based phylogeny, we also performed the first inclusive biogeographic reconstruction of the Boletaceae and assessed morphological trait evolution. Overall, we provide new insights into the broad patterns of evolution of this enigmatic fungal group.

MATERIALS AND METHODS

Sampling.—Taxon selection focused on obtaining representatives of all currently accepted genera, selecting type species whenever possible. Because the current understanding of genera is incomplete and rapidly changing, we could not include representatives of all currently accepted genera that were published during the course of this study. Specimens from geographic regions unrepresented in prior studies were also

included. A total of 418 Boletaceae specimens were gathered from a global distribution using collections made by the authors, those borrowed from four institutions, and donations from citizen scientists (SUPPLEMENTAL TABLE 1). In addition, we utilized genome data publicly available from the JGI Mycocosm Portal (Grigoriev et al. 2014) for *Boletus coccyginus*, *B. reticuloceps*, *Butyriboletus roseoflavus*, *Chiua virens*, *Lanmaoa asiatica*, and *Imleria badia* (Miyauchi et al. 2020, Wu et al. 2022, Kohler et al. 2015). *Paxillus involutus*, *Paxillus adelphus*, and *Hydnomerulius pinastri* genomes from JGI were used for outgroups (Kohler et al. 2015).

DNA extraction and sequencing. —Genomic DNA was extracted in one of three ways. 1) 10 mg of hymenophore tissue from each specimen was homogenized in 2.0 ml screw-cap tubes containing a single 3.0 mm and 8 x 1.5 mm stainless steel beads using a BeadBug™ microtube homogenizer (Sigma-Aldrich, #Z763713) for 120 seconds at a speed setting of 3500 rpm. After physical disruption, DNA was extracted using the Monarch® Genomic DNA Purification Kit (New England Biolabs, Massachusetts; #T3010) with the Monarch® gDNA Tissue Lysis Buffer (#T3011) using double the volume of lysis buffer, one hour lysis incubation at 56 C , and 550 µl of wash buffer during each of the wash steps. 2) an in-house 96-well plate protocol where tissue is physically homogenized, as above, after which 1000 µL of lysis buffer (1% sodium dodecyl sulfate, 10 mM Tris, 10 mM EDTA, 5mM NaCl, 50mM dithiothreitol, pH 8.0) is added. To this solution is added 4 µL of RNAse A (20 mg/mL), the solution is vortexed, and then incubated at 37 C for 10 min. Next, 10 µL of proteinase K (20 mg/mL) is added, the solution vortexed, and then incubated at 56 C overnight on an Eppendorf ThermoMixer® with agitation at 400 rpm. After lysis, the tubes are centrifuged at max speed (17,000 x g) to pellet the cellular debris. 700 µL of supernatant is removed to a new 1.7 mL microcentrifuge tube with hinged cap to which

150 162.5 µL 3.0 M potassium acetate (pH 5.5) is added. The solution is mixed briefly and
151 then put on ice for five min, followed by a second centrifugation, as above. Avoiding
152 the pellet, the supernatant is removed to a well of a 96-well 10 µM filter plate
153 (Enzymax, #EZ96FTP) set in a 2 mL MASTERBLOCK® collection plate (Grainer,
154 #780271). Filtration is achieved through centrifugation at 1500 x g for 2 min. The flow-
155 through is transferred to a new 1.7 ml microcentrifuge tube with hinged cap and
156 centrifuged, as above. Without disturbing the pellet, the supernatant is removed to a
157 new 2.0 mL microcentrifuge tupe with hinged cap and 1000 µL of binding buffer (5M
158 guanidium hydrochloride, 40% isopropanol) is added and the solution homogenized by
159 pipetting. The binding solution is then transferred to a well of a 96-well long-tip
160 AcroPrep™ Plate (PALL, #8133) that was pre-conditioned by pulling 400 µl Tris-HCl
161 buffer (pH 8.0) through using a vacuum manifold. DNA is bound to the filter by
162 centrifugation at 1500 x g for 2 min or using a vacuum manifold. The filter is washed
163 twice with 700 µl of wash buffer (20% solution of 80mM NaCl, 8mM Tris-HCl, pH 7.5
164 and 80% ethanol) using centrifugation or vacuum, and then the filter is dried with
165 centrifugation at 1500 x g for 15 min. Residual ethanol is removed by incubating the
166 filter plate at room temperature for 30 min. To elute the DNA from the filter, 50 µl of
167 elution buffer (0.1x Tris-EDTA buffer, pH 8-9) prewarmed to 60 C is added directly to
168 the filter, incubated for 2 min at room temperature, and eluted into a new 2 ml
169 MASTERBLOCK® collection plate with centrifugation at 1500 rpm for 2 min. The
170 elution step is repeated once. 3) a phenol-chloroform DNA extraction protocol where
171 tissue is physically homogenized, as above, and lysed using the Tissue Lysis buffer
172 from the Monarch® Genomic DNA Purification Kit (NEB, #T3010S) with double the
173 volume of lysis buffer and a 1 h incubation at 56 C. Then, total lysate was placed in
174 Phase Lock Gel™ Light tubes (QuantaBio, #2302820) along with an equal volume of

OmniPur® Phenol:Chloroform:Isoamyl Alcohol (25:24:1, TE-saturated, pH 8.0) solution (MilliporeSigma, Calibiochem #D05686) and then mixed by gentle inversion for 15 minutes using a fixed speed tube rotator. After mixing, tubes were centrifuged at maximum speed (14,000 x g) for 10 minutes, then the aqueous (top) layer was transferred to a new phase-lock gel tube and the process repeated. DNA precipitation of the aqueous phase was performed by adding 5M NaCl to a final concentration of 0.3M and two volumes of room temperature absolute ethanol, inverting the tubes 20x for thorough mixing followed by an overnight incubation at -20C. DNA was pelleted by centrifugation at 14,000 x g for 5 min, washed twice with freshly prepared, ice cold 70% ethanol, air-dried for 15 min at room temperature, and then resuspended in 150 µl of Elution Buffer from the Monarch® Genomic DNA kit.

DNA extract quality was assessed for quality using a NanoDrop 1000 (Thermo Scientific) and fragment integrity using agarose gel electrophoresis. Genomic DNAs were sequenced using a combination of paired-end sequencing on the Illumina MiSeq, HiSeq, and Novaseq sequencing platforms (SUPPLEMENTARY TABLE 2). All raw reads and whole genome assemblies are deposited in the Short Read Archive (Bioproject#PRJNA1022813).

Genome assembly, ortholog extraction and phylogenetic analysis. —Raw sequencing reads were quality-filtered and adapter-trimmed using fastP v0.20.1 (Chen et al. 2018) with default settings. Genome assemblies were produced from quality-filtered reads using SPAdes v3.15.0 (Bankevich et al. 2012) with five k-mer values (k=77,85,99,111,127). From each genome, we identified 1764 highly conserved single copy orthologs using BUSCO with the “basidiomycota odb 10” dataset. Orthogroups that were present in less than 75% of taxa and taxa with less than 20% ortholog recovery were removed. Retained orthologs were aligned using MAFFT v7.397 (Katoh,

Rozewicki, and Yamada 2017) with the "L-INS-I" algorithm, and maximum- likelihood gene-trees were inferred using IQ-TREE v2.0.3 (Minh et al. 2020) with automatic model selection in ModelFinder (Kalyaanamoorthy et al. 2017) and ultrafast bootstrapping (BS, (Hoang et al. 2018)) with 1000 replicates. A summary coalescent species tree was constructed from the resulting gene trees using hybrid- ASTRAL implemented in ASTER (v1.15) (Zhang and Mirarab 2022). Branch lengths in substitutions/site were estimated under maximum likelihood on the species tree using the "-te" option in IQ-TREE, with a partitioned concatenated alignment of all BUSCO genes used in species tree construction.

Gene tree comparison. —To evaluate discordance, individual gene trees were compared using six metrics calculated in SortaDate (average bootstrap support, clocklike branch lengths, tree length; Smith et al. 2018) and the R package 'TreeDist' (generalized Robinson-Foulds metrics; Smith 2020, 2022). In addition to data matrix summaries (number of taxa, alignment length), Pearson's correlations were calculated to determine relationships between metrics.

Divergence dating. —A timetree was inferred by applying the RelTime method (Tamura et al. 2012, 2018) conducted in MEGA11 (Stecher et al. 2020, Tamura et al. 2021) to the species tree with ML-estimated branch lengths. To reduce computational burden, time-calibrated branch lengths were calculated using the Maximum Likelihood (ML) method and the General Time Reversible substitution model (Nei and Kumar 2000) from two sets of 100 genes: 1) the top 100 genes with well-supported clock-like trees determined using SortaDate (Smith et al. 2018) and 2) the top 100 genes with the smallest generalized Robinson-Foulds ('gRF') distances to the species tree calculated using the R package 'TreeDist.' The timetree was computed using two sets of calibration constraints. The first included two calibrations: 1) a secondary calibration

for the stem age of the Boletaceae from 50-150 mya (Varga et al. 2019, Wu et al. 2022) and 2) a secondary calibration for the stem age of *Boletus edulis* from 5-13 mya (Tremble et al. 2022). The second set included the former two calibrations plus four of the five internal calibrations using the highly supported core shifts from Varga et al. (2019). Because many of the clades in Varga et al. were incongruent with our topology, calibrations were selected using the most inclusive node, except for *Aureoboletus* which could not be reconciled with our results. The Tao et al. (2020) method was used to set minimum and maximum time boundaries on nodes for which calibration densities were provided, and to compute confidence intervals. Outgroup node ages were not estimated because the RelTime method uses evolutionary rates from the ingroup to calculate divergence times and does not assume that evolutionary rates in the ingroup clade apply to the outgroup.

Ancestral state reconstruction. — Morphological/macrochemical traits were coded according to original descriptions and verified with microscopic analysis when traits were ambiguous. Four traits were scored as binary or multistate characters: 1) hymenophore anatomy (straight tubes = 0, tubular with cross walls = 1, lamellate = 2, not applicable = 3), 2) color changes from damage (none = 0, blue = 1, black/brown = 2, not applicable = 3), and sporocarp morphology (pileate-stipitate with exposed hymenophore = 0, secotioid = 1, gasteroid = 2), 4) spore ornamentation (smooth = 0, not smooth = 1) (SUPPLEMENTARY TABLE 4). The state of hymenophore anatomy defined as “tubular with cross walls” refers to hymenophores that have tubes at two or more lengths, giving the appearance of a primary long tube with shorter internal cross-walls. A “not applicable” category was scored for hymenophore anatomy and color changes from damage to accommodate secotioid/gasteroid taxa and taxa with unknown changes, respectively. An alternative coding scheme for sporocarp morphology was also

used in an attempt to disentangle the transition between pileate-stipitate and gasteroid morphologies from the loss of ballistospory. In this alternative coding scheme, two binary traits were scored: stipe (present = 0, absent = 1) and ballistospory (no = 0, yes =1). Ancestral state reconstruction of the root node of the Boletaceae was implemented with BayesTraits V4.0.0, using the MCMC approach over 1,100,000 iterations, with a "burn-in" of 100,000 iterations (Mead and Pagel 2022). Model convergence was assessed with the program Tracer (v1.7.1, Rambaut et al. 2018), and determined as an effective sample size (ESS) of >300 for all variables.

Ancestral Range Reconstruction. —Numerous analytical methods for reconstructing historical biogeography exist, accounting for processes such as vicariance, dispersal, and cladogenesis (Ronquist 1994; Ree et al. 2005; Landis et al. 2013). To account for these macroevolutionary processes in our ancestral state reconstruction in the Boletaceae, we utilized BioGeography with Bayesian (and likelihood) Evolutionary Analysis with R Scripts ("BioGeoBEARS"; Matzke 2018). Samples were coded in two ways: 1) Paleotropical (consisting of Africa and tropical Asia), Neotropical (South and Central America), South Temperate (temperate Australia and New Zealand), or North Temperate (North America, Europe, northern temperate Asia), and 2) by these floristic regions: Holarctic including Central America, Neotropical, Chilean-Patagonian, African, Indo-Malesian, Australian, and Novo-Zealandic (Liu et al 2023) (SUPPLEMENTARY TABLE 3). Central America was combined with the Holarctic region as Central American ECM fungi are mostly derived from North American ancestors (Halling 1996). The most likely model was chosen according to AIC and weighted AIC score calculated in BioGeoBEARS.

RESULTS

DNA sequencing, genome assembly, and ortholog extraction. —Whole genome sequencing of 418 specimens resulted in 13,794,532 paired-end reads per specimen on average (SUPPLEMENTAL TABLE 2). On average, genome assemblies possessed an assembly N50 of 12.9 Kbp (thousand base-pairs), total assembly length of 61.6 Mbp (million base-pairs), 53,972 scaffolds, and a BUSCO score of 74.7%. 34 of 418 specimens possessed BUSCO scores less than 20%, and 175 specimens possessed BUSCO scores greater than 90% (SUPPLEMENTARY TABLE 2). After removing specimens with poor BUSCO recovery, our final dataset included 383 Boletaceae specimens, three outgroup taxa, and 1461 single-copy orthologs.

Phylogenetic analysis. — The summary coalescent tree resolved most nodes with strong support (FIG. 2). Many of the groups recovered are consistent with previous studies but now with statistical support (Dentinger et al. 2010, Nuhn et al. 2013, Wu et al. 2014). We recognized the six subfamilies following previous authors (Wu et al. 2014), which led us to formally recognize two new subfamilies (Tremble et al. 2023). Many of the currently accepted genera that are not mono- or oligo-typic are polyphyletic. One notable pattern is the phylogenetic placements of the endemic Chilean taxa, all of which were recovered as ancient lineages of similar age within four of the subfamilies: *Gastroboletus valdivianus* in Xerocomoidae, *Boletus loyita* in Austroboletoidae, *Boletus loyo* in Suillelloidae, and *Boletus putidus* in Boletoidae.

Gene tree comparison. —Average bootstrap support had the highest positive correlation with the number of taxa present (Pearson's coefficient = 0.76), and weak to moderate negative correlations with alignment length (Pearson's coefficient = -0.17), clocklike branch lengths (Pearson's coefficient = -0.13), and total tree length (Pearson's coefficient = -0.20). Generalized Robinson-Foulds distances were weakly to moderately negatively correlated with number of taxa (Pearson's coefficient = -0.33), total length

(Pearson's coefficient = -0.30), and clocklike branch lengths (Pearson's coefficient = -0.13), and weakly to moderately positively correlated with alignment length (Pearson's coefficient= 0.29) and average bootstrap support (Pearson's coefficient = 0.17). Clocklike branch lengths and total tree length were weakly positively correlated (Pearson's coefficient= 0.15).

Divergence dating. — Using the two- and six-calibration sets the following ages were estimated (FIGS. 2, 3). Stem ages for the Boletaceae were estimated at 138-139 mya and 77 mya. The crown age of the Boletaceae and origin of Chalciporoideae was estimated at 103-105 mya and 63 mya (49-77 mya). The stem age of the Phylloboletelloideae was estimated at 83-87 mya and 58 mya (49-77 mya)., The radiation of the remaining subfamilies was estimated to have occurred between 61 and 51 mya. The origin of *Boletus* sensu stricto (i.e. "true porcini") was estimated at 38 mya and 35 mya (29-42 mya), and its diversification was estimated at 29-30 mya and 26 mya (20-34 mya).

Ancestral state reconstruction. —Ancestral state reconstruction with Bayestraits achieved strong convergence (all variables with ESS > 300) and recovered the most likely ancestor of the Boletaceae to have a pileate-stipitate, lamellate sporocarp with ornamented basidiospores. The highest transition rates were observed in changes from secotioid to gasteroid and from secotioid to pileate-stipitate morphologies. Secotioid morphology appeared to be a relatively transient evolutionary state (TABLE 1). High transition rates were also found to occur from gasteroid to pileate-stipitate morphology, supporting evidence for the reversibility of gasteromycetization.

Ancestral range reconstruction. —Ancestral distribution reconstruction recovered a likely Paleotropical origin of the Boletaceae (DEC+J model chosen with lowest AIC and AICc for both coding sets), with two major descendant radiations originating in the

Paleotropics (Africa and Asia) and Neotropics (FIG. 3). In addition, we found evidence for multiple diversification events spurred by the separation of Gondawana (FIG. 3). Gondwanan separation occurred in two predominant phases: Phase 1, which involved the separation of Southern South America, Southern Africa, Australia-Antarctica, and Madagascar-India, beginning approximately 180 mya and largely completed by 120 mya (Jokat et al. 2003) and Phase 2, involving the separation of South America and Africa, which was completed 80 mya (Reguero and Goin 2021). At the split between the Austroboletoidae and Suillelloidae (FIG. 3), we estimated a putative Phase 1 Gondwanan separation to have occurred 150-120 mya, which led to rapid formation of South Temperate, Neotropical, and Paleotropical lineages. Later, around 90-70 mya, at least five putative Phase 2 separation events occurred, splitting the Paleotropical and Neotropical lineages.

In our four category paleo-region coding set, the Boletaceae ancestor was equally likely to be Neotropical or Paleotropical. However, the subsequent node that leads to the rest of the Boletaceae (excluding Phyllobolletoidae and Chalciporoideae) was well-supported as Paleotropical, as were all immediate descendent nodes. Our coding of the Chalciporoideae and the single *Phylloboletellus* specimen likely had a strong influence on deep-node ancestral range reconstructions. The backbone nodes of the Boletaceae excluding Phylloboletoidae and Chalciporoideae were estimated as Asian in origin, corroborating the four-category analysis, though with less confidence. Migrations between phytogeographic regions were dominated by dispersals between the Indo-Malesian and Holarctic regions (FIGS. 3,4).

DISCUSSION

The fully resolved phylogeny supports the recognition of eight subfamilies, including the newly defined Phylloboletelloideae and Suillelloideae (Tremble et al. 2023). The

subfamilial relationships were resolved for the first time. The Chalciporoideae was recovered as the earliest diverging group in the Boletaceae, a relationship previously noted by Wu et al. (2014). The enigmatic *P. chloephorus* (Singer and Diglio 1952) was the next lineage to branch off before the radiation that gave rise to the six additional subfamilies. Previous studies have placed *Pseudoboletus parasiticus* in a position similar to that of *P. chloephorus* in our study (Nuhn et al. 2013, Wu et al. 2014, Sato and Toju 2019, Caiafa and Smith 2022). We were, however, unable to include a representative of *P. parasiticus* in our study so cannot corroborate its putative phylogenetic position.

The tree topology has intriguing implications for the role of ecological transitions in Boletaceae diversification. Members of the earliest-diverging Chalciporoideae species can be facultatively ECM, saprotrophic or mycoparasitic (Caiafa and Smith 2022) and *P. chloephorus* may not be ECM given its occurrence in non-ectotrophic forests (Singer and Diglio 1952). Moreover, *P. parasiticus* and other *Pseudoboletus* spp. produce sporocarps directly attached to gasteroid *Scleroderma* and *Astraeus* and are assumed to be mycoparasites (Raidl 1997; Binder and Hibbet, 2006; Nuhn et al. 2013). Altogether, the basal position of these early diverging groups suggests that the ancestor of the Boletaceae was likely saprotrophic and not ECM. This possibility is in line with the results of Sato and Toju (2019) which indicated that the ECM habit emerged with the origin of the six derived Boletaceae subfamilies. Genomic changes coinciding with the emergence of an obligate ECM habit further support the view that this nutritional shift has profoundly impacted Boletaceae (Wu et al. 2022).

Many taxonomic changes in the Boletaceae have been proposed in recent years. In particular, new genera have been erected for phylogenetically unresolved lineages. Many of these new genera are mono- or oligo-typic (composed of one or few species)

(e.g. Castellano et al. 2016; Chakraborty et al. 2015; Henkel et al. 2016; Halling et al. 2023). This proliferation of new genera has made it difficult or impossible to recognize inclusive groupings without requiring knowledge of the species. On the bright side, the strong nodal support throughout our phylogeny sets the stage for a new, comprehensive and stable generic-level taxonomy. We will address this in subsequent works when all recently described genera are represented.

Our biogeographic and divergence dating analyses support a Gondwanan origin of the Boletaceae. Subsequent divergence was likely facilitated by continental drift-based vicariance events and possible long-distance dispersals. Other recent studies have shown that lineages of ECM fungi originated in Gondwana or more recently in paleotropical regions (Hosaka et al. 2008, Matheny et al. 2009, Dentinger et al. 2010, Ryberg and Matheny 2011, Kennedy et al. 2012, Sanchez-Ramirez et al. 2015, Han et al. 2018; Hackel et al. 2022; Codjia et al. 2023). Phytogeographic endemism was implied with our biogeographic reconstruction. The strongest migrations occurred recently over the past 50 my between the Indo-Malesian and Holarctic regions. We acknowledge the difficulty to determining origins and dispersal events in the absence of fossils or other corroborating evidence. Nonetheless our study and others suggest that vicariance may have played a strong role in the distribution of ECM fungal taxa, despite the long-distance dispersal capacity of airborne spores (Matheny et al. 2009, Peay et al. 2010, Peay and Matheny 2016). Conversely, pure vicariance cannot explain the close phylogenetic relationships seen between distantly disjunct taxa. Long-distance dispersals may have occurred, albeit rarely. While long-distance dispersal is demonstrably possible in the Boletaceae and other ECM lineages the likelihood of its frequent occurrence is low (Geml et al. 2012; Hackel et al. 2022; Tremble et al. 2022). Most basidiospores do not travel far from the parental sporocarp (Galante et al. 2011),

399 and the probability of two airborne basidiospores landing in close-enough proximity to
400 mate is negatively correlated with increasing distance from sporocarps (Peay et al.
401 2012; Golan and Pringle 2017). Such improbabilities notwithstanding, our
402 biogeographic patterns are consistent with episodic long-distance dispersal, possibly by
403 aerial dispersal of basidiospores, spores vectored by migrating animals (e.g., Elliot et al.
404 2019) or somatic mycelia on rafting vegetation (Thiel et al. 2005).

405 Our biogeographic reconstructions are consistent with the "Southern Route to
406 Asia" hypothesis (Wilf et al. 2019). This idea proposes that ECM Fagaceae and their
407 symbiotic fungi originated in Gondwana and were carried on Australia north to Asia. In
408 this scenario the Gondwanan ECM habitat tracked climatic niches on the desertifying
409 continent northward as the Australian plate collided with the Pacific plate. A relictual
410 ECM community remained in a newly isolated New Guinea and subsequently spread
411 northwest along the montane Australasian archipelago, followed by dispersal into
412 continental Asia. Many of the dispersal events we found between Indo-Malesia and
413 other regions, especially the Holarctic, are inferred within the last 20 my, coincident
414 with the late-Oligocene collision of Australia with the Pacific plate (Hall 2011). As
415 suggested by Halling et al. (2011) recent Boletaceae migrations likely occurred across
416 the Australasian archipelago and are corroborated by our inferred recent regional
417 dispersal events.

418 Biogeographic reconstructions are highly sensitive to taxon sampling and our
419 dataset is not immune to equivocal reconstructions. For example, in both coding
420 schemes the ancestral node of the Chalciporoideae had the highest probabilities of a
421 North Temperate and North American origin, respectively. However, with no
422 Chalciporoideae samples from Asia, Africa or Australia/New Zealand in our study, their
423 potential impacts on the reconstruction are unknown. Such sampling gaps

notwithstanding, we have the most geographically comprehensive sampling for Boletaceae ever compiled and provide the first opportunity to examine global-scale biogeographic patterns. Insights into the evolution of the Boletaceae are revealed for the first time, despite mild uncertainty at a minority of nodes.

The evolutionary origins of distinctive regional Boletaceae assemblages have long been a mystery (Horak 1977). For example, the endemic Boletaceae of Chile and Argentina have not been included in previous phylogenetic studies, and their morphology-based affinities have been inconclusive (Horak 1977). The recovery of several Chilean species as ancient lineages in four of the subfamilies implies that they have survived in isolation without speciating for millions of years. The closest relatives of these Chilean boletes occurred in geographic regions as disjunct as North America, lowland tropical northern South America, and Australia. *Boletus loyita* and *G. valdivianus* were most closely related to extant Australian taxa, suggesting an origin prior to final Gondwanan disarticulation (Reguero and Goin 2021). Close relationships between southern Gondwanan Australian and southern South American taxa have been documented elsewhere (Feng et al. 2017). In all likelihood Chilean boletes arose in Gondwana, separated from their sister lineages during Gondwanan disarticulation, and underwent no subsequent speciation for tens of millions of years.

Ancestral range reconstruction recovered an Asian origin of the core, “true porcini” genus *Boletus* s. str. as previously suggested (Feng et al. 2012). However, we cannot entirely rule out an African origin. The Central African endemic *Boletus alliaceus* was recovered here as a sister taxon to *Boletus* s. str., and a similar relationship was found for the recently described *Paxilloboletus africanus* (Badou et al. 2022). Furthermore, we estimated the origin of *Boletus* s. str to be 40 mya, which may indicate why the sister lineages to *Boletus* s. str. are endemic to Africa. India had

449 separated from Africa and Madagascar ~120 mya (Reguero and Goin 2021), and at 40
450 mya was already colliding with Asia (Aitchison et al. 2007; Hu et al. 2016). If *B.*
451 *alliaceus* and *P. africanus* are indeed sister lineages of *Boletus* s. str., then the arrival
452 and subsequent diversification of true porcini in Asia must have been a dispersal event,
453 because the separation of India from mainland Africa ~180-170 mya (Hankel 1994)
454 occurred long before our estimated age of the *Boletus* s.s. ancestor (~40 mya). Even if a
455 more recent ancestor existed in Madagascar or the Seychelles, the separation of India
456 from these landmasses at ~90 mya (Storey et al. 1995) and ~64 mya (Norton and Sclater
457 1979), respectively, is still much older than our current age estimates for true porcini.
458 Furthermore, most or all ECM fungi in Madagascar appear to have arrived on the island
459 through dispersal its separation from Africa (Rivas-Ferreiro et al. 2023), so dispersal is
460 the most plausible mechanism unless ancient Malagasy relict taxa are discovered. In the
461 current study currently undescribed species of *Boletus* s. str. were recovered from
462 Taiwan, Malaysian Borneo, and the Gulf Coast of the US, indicating that much more
463 diversity exists in the genus. To sort out the origins and full diversity of *Boletus* s. str.
464 more mycological exploration and whole genome sequencing are needed. In particular,
465 discovery and analysis of true porcini basal lineages from India and Africa could shed
466 further light on the origin of this charismatic group.

467 Divergence dating estimated the origin of the Boletaceae at 138-139 mya, and
468 ancestral range reconstructions suggested it may be even older. Ranking genes with
469 different metrics had little impact on divergence date estimates. However, the two
470 calibrations sets gave very different estimates for most nodes. The estimated origin
471 dates of the Boletaceae using the Varga et al. (2019) calibrations were almost half those
472 of the two-calibration set. It is difficult to interpret these wildly different divergence
473 dates given the lack of fossil evidence. However, the dates estimated using the Varga et

al. (2019) calibrations are suspect due to extensive topological incongruence of their phylogenetic trees with ours. Our older divergence estimate corroborates the results of He et al. (2020) and our internal dates correspond with other results, such as the ~48 mya origin of the *Strobilomyces* group (Han et al. 2018). Our older divergence estimate is also in line with the origin of ECM Pinaceae in the early Cretaceous (Brundrett and Tedersoo 2018). Therefore, we consider the older estimate to be more accurate.

In our ancestral range reconstruction analysis, we found evidence of multiple diversification events that may have been initiated by Gondwanan breakup. The first phase of the Gondwanan separation postulated by Jokat et al. (2003) correlates well with our estimated origin of the Boletaceae and indicates that the family was diverse and widely distributed by 120 mya, substantially older than the estimated age from our divergence dating analysis but within the 95% confidence interval. Our dates are at best coarse estimates based on fossil-free secondary calibrations. However, the phylogenetic pattern of vicariance that parallels the breakup of Gondwana is compelling and offers corroborating evidence that our estimated ages may in fact be too young. In any case, our divergence estimates suggest that the Boletaceae originated and diversified within the early to late Cretaceous period. During this time global climate was warm and wet (Hay and Floegal 2012), gymnosperms and subsequently angiosperms diversified (Crisp and Cook 2011), and the supercontinental land masses broke apart (Jokat et al. 2003).

The Boletaceae mostly consists of species that form ECM assocations, but emerging evidence suggests the ancestor may have had mycoparasitic capacity. The gain of obligate ECM ecology in the six most-derived subfamilies likely occurred after their divergence from the Phylloboletelloidae. *Phylloboletellus chloephorus* is from non-ECM dominated habitats. The Chalciporoideae have not been definitively shown to form ECM associations but do have saprotrophic or mycoparasitic capacities (Caiafa et

al. 2022). While mycoparasitic *Pseudoboletus* species have also been recovered as early-diverging Boletaceae lineages (Nuhn et al. 2013, Sato and Toju 2019, Cortes-Perez et al. 2023) and may have close affinities with lamellate *Phylloboletellus*, we were not able to evaluate *Pseudoboletus* in this study. A more thorough investigation of the ecology of early-diverging Boletaceae is needed to test this "mycoparasitic origin" hypothesis.

A longest standing debate among Boletaceae systematists has centered on the utility of morphological traits for defining natural genera. Basidiospore color, ornamentation, and hymenophore arrangement were long emphasized in this respect. These features have been used as evidence for dividing the Boletaceae into multiple genera (e.g., Singer 1945a,b; 1947; Pegler and Young 1981) or treating nearly all Boletaceae as a single genus (Corner 1972). More recently, hyphal anatomies of sporocarp structures and pigment chemistry have been emphasized (e.g. Binder et al. 2002; Šutara 2005). Yet, despite the morphological and chemical variability in the Boletaceae, the family is typified by the 'bolete' macromorphology of fleshy, pileate-stipitate sporocarps with tubular hymenophores. In addition, type of basidiospore ornamentation has been long considered to be a genus-unifying trait in genera such as *Strobilomyces*, *Boletellus*, and *Austroboletus* (Berkeley 1851, Murrill 1909, Corner 1972, Pegler and Young 1981, Wolfe 1980). Despite such traditional views, our ancestral state reconstructions suggest that the ancestor of the Boletaceae had a pileate-stipitate sporocarp with a lamellate hymenophore and ornamented basidiospores. This likely resulted from the basal phylogenetic position of the lamellate *P. chloephorus* (Singer and Diglio 1952).

The evolution of sequestrate morphologies has long been thought to be irreversible (Thiers 1984). The transition from pileate-stipitate to secotioid to gasteroid

morphology involves enclosure of the hymenophore and loss of ballistospory, which are unlikely to be regained once lost (Hibbett et al. 1997, Hibbett 2004, Sanchez-Garcia et al. 2020). However, prior studies have not fully rejected the hypothesis that gasteromycetization is irreversible (Hibbett 2004; Wilson et al. 2011; Sanchez-Garcia et al. 2020). Our ancestral state reconstructions under two coding schemes strongly supported transition to and from gasteroid forms. This suggests that gains or losses of ballistospory may also be reversible conditions. In our analyses, transitions between pileate-stipitate with exposed hymenophore, secotioid, and gasteroid forms suggest that the secotioid condition is intermediate, as indicated by the equal rates of transition to gasteroid and pileate-stipitate forms. Moreover, inferred transition rates from pileate-stipitate to both secotioid and gasteroid forms were almost zero, suggesting that the secotioid condition is evolutionarily unstable. This result contrasts with the stability of *Cortinarius* secotioid taxa suggested by Peinter et al. (2001). A plausible hypothesis is that a membranous partial veil that covers the hymenophore at early stages of sporocarp development may predispose it to gasteromycetization. However, although we did not test this explicitly, based on the phylogenetic distribution of taxa with membranous veils (e.g., *Pulveroboletus*, *Veloporphyrellus*), it is clear that the membranous partial veil is a convergent trait not closely associated with secotioid or gasteroid morphologies. A possible exception to this is *Veloboletus limbatus*, which is most closely related to the gasteroid *Gastroboletus valdivianus*, although their common ancestor was estimated at ~40 mya.

Transitions between hymenophore organization parallels the sporocarp morphologies. The “tubular with crosswalls” hymenophore condition appears to be intermediate between lamellate and tubulate forms, with transitions to tubes being 1.3-5.8 times greater than the opposite transitions. However, the greatest transition rate was

549 from lamellate directly to tubulate forms, indicating that an intermediate morphology
550 may not be necessary or, like the secotioid condition, may be evolutionarily unstable.
551 Our data provide compelling evidence that lamellate hymenophores, color changes, and
552 gasteromycetization have evolved multiple times in the Boletaceae and are reversible.

553 **SUMMARY**

554 The Boletaceae underwent a rapid radiation and subsequent long period of phylogenetic
555 instability. These issues had long prevented accurate assessment and analysis of trait
556 evolution and conclusive generic-level taxonomic frameworks in the family. Previous
557 molecular phylogenetic studies were based on a limited taxon sampling and a few loci
558 and generated trees with many short branches and little deep-node support. This study
559 provides the first Boletaceae phylogeny with strong support at deep nodes, based on a
560 massive dataset of 1461 single copy genes from 383 genomes sampled from
561 taxonomically and geographically comprehensive specimens. Our analyses indicated
562 that the Boletaceae likely arose before Gondwanan breakup and that present-day
563 distributions are partly due to vicariance. Long-distance dispersal could not be ruled out
564 for some current distributions. Morphological traits resulted from convergence and
565 frequent reversals, which, along with rapid radiation, have long confounded attempts to
566 achieve a natural intrafamilial classification. This study provides new genomic data and
567 a solid phylogenetic framework that will enable a renewed foundational taxonomy as
568 well as deeper analysis of trait evolution.

569 **AKNOWLEDGEMENTS**

570 This work was supported by NSF-DEB awards DEB-2114785 to BD and DEB-0918591
571 to TWH and DEB-1556338 to TWH and BD; National Geographic Society's
572 Committee for Research and Exploration grants (6679-99, 7435-03, and 8481-08 to
573 TWH). JMM was supported by grants from the ROM Governors and the Natural

574 Sciences and Engineering Research Council of Canada, Discovery Program. We would
575 like to thank Dr. Roy Halling for the numerous specimens provided.

576 **CONFLICTS OF INTEREST**

577 The authors declare no conflict of interest, financial or otherwise.

578 **LITERATURE CITED**

579 Aitchison JC, Ali JR, and Davis AM. 2007. When and where did India and Asia
580 collide? Journal of Geophysical Research: Solid Earth. 112:B5
581
582 Arora D. 2008. California porcini: three new taxa, observations on their harvest, and the
583 tragedy of no commons. Economic Botany. 62:356–375.
584
585 Badou SA, Furneaux B, De Kesel A, Khan FK, Houdanon RD, Ryberg M, Yorou NS.
586 2022. *Paxilloboletus* gen. nov., a new lamellate bolete genus from tropical Africa.
587 Mycological Progress. 21:243–256.
588
589 Bankevich A, Nurk S, Antipov D, Gurevich AA, Dvorkin M, Kulikov AS, Lesin VM,
590 Nikolenko SI, Pham S, Prjibelski AD, Pyshkin AV, Sirotkin AV, Vyahhi N, Tesler G,
591 Alekseyev MA, and Pevzner PA. 2012. SPAdes: a new genome assembly algorithm and
592 its applications to single-cell sequencing. Journal of Computational Biology. 19:455–
593 477.
594
595 Berkeley MJ. 1851. Decades of fungi. Decade XXXIV. Sikkim-Himalayan fungi
596 collected by Dr. Hooker. Hooker's Journal of Botany and Kew Gardens Miscellany.
597 3:77—84.
598

599 Binder M, Bresinsky A. 2002. *Retiboletus*, a new genus for a species-complex in the
600 Boletaceae producing retipolides. Feddes Repertorium. 113:30–40.
601
602 Binder M, Hibbet DS. 2006. Molecular systematics and biological diversification of
603 Boletales. Mycologia. 98:971–981.
604
605 Brundrett MC, Tedersoo L. Evolutionary history of mycorrhizal symbioses and global
606 host plant diversity. New Phytologist. 220:1108–1115.
607
608 Bruns TD, Palmer JD. 1989. Evolution of mushroom mitochondrial DNA: *Suillus* and
609 related genera. Journal of Molecular Evolution. 28:349–362.
610
611 Bruns TD, Vilgalys R, Barns SM, Gonzalez D, Hibbett DS, Lane DJ, Simon L, Stickel
612 S, Szaro TM, Weisburg WG, Sogin ML. 1992. Evolutionary relationships within the
613 fungi: analyses of nuclear small subunit rRNA sequences. Molecular Phylogenetics and
614 Evolution. 1:231—241.
615
616 Caiafa MV, Smith ME. 2022. Polyphyly, asexual reproduction and dual trophic mode in
617 *Buchwaldoboletus*. Fungal Ecology. 56:101—141.
618
619 Castellano MA, Elliott TF, Truong F, Séné O, Dentinger BTM, Henkel TW. 2016.
620 *Kombocles bakaiana* gen. sp. nov. (Boletaceae), a new sequestrate fungus from
621 Cameroon. IMA Fungus. 7: 239–245.
622

623 Chakraborty D, Das K. 2015. A new generic record of Boletaceae for Indian mycobiota.
624 Current Research in Environmental & Applied Mycology. 5:138–144.
625
626 Chen S, Zhou Y, Chen Y, Gu J. 2018. fastp: an ultra-fast all-in-one FASTQ
627 preprocessor. Bioinformatics. 34:884–890.
628
629 Codjia JEI, Sánchez-Ramírez S, Ndolo Ebika ST, Wu G, Margaritescu S, Komura DL,
630 Oliveira JJS, Ryberg M, Tulloss RE, Yorou NS, Moncalvo JM, Yang ZL. 2023.
631 Historical biogeography and diversification of ringless *Amanita* (section *Vaginatae*)
632 support an African origin and suggest niche conservatism in the Americas. Molecular
633 Phylogenetics and Evolution. 178:107644.
634
635 Corner EJH. 1972. Boletus in Malaysia. The Botanic Gardens Singapore. The
636 Government Printer. 263pp
637
638 Cortés-Pérez A, Ramirez-Guillen F, Garcia-Jimenez J, Ramirez-Cruz V, Villalobos-
639 Arambula AR, Reynaga DMB, Guzman-Davalos L. 2023. *Pseudoboletus silvaticus*
640 (Boletaceae, Basidiomycota), a new species from Mexico. Phytotaxa. 589:27–38.
641
642 Crisp MD and Cook LG. 2011. Cenozoic extinctions account for the low diversity of
643 extant gymnosperms compared with angiosperms. New Phytologist. 192:997—1009.
644
645 Das K, Chakraborty D, Baghela A, Singh SK, Dentinger BTM. 2015. *Boletus*
646 *lakhanpalii*, a new species in Boletaceae from Sikkim India with uncertain phylogenetic
647 placement. Sydowia. 67:11–19.

Das K, Chakraborty D, Baghela A, Singh SK, Dentinger BTM. 2016. New species of xerocomoid boletes (Boletaceae) from Himalayan India based on morphological and molecular evidence. Mycologia. 108:753–764.

Dentinger BTM, Ammirati JF, Both EE, Desjardin DE, Halling RE, Henkel TW, Moreau PA, Nagasawa E, Soytong K, Taylor AF, Watling R, Moncalvo JM, McLaughlin DJ. 2010. Molecular phylogenetics of porcini mushrooms (*Boletus* section *Boletus*). Molecular Phylogenetics and Evolution. 57:1276–1292.

Dentinger BTM, Gaya E, O'Brien H, Suz LM, Lachlan R, Diaz-Valderrama JR, Koch RA, Aime MC. 2016. Tales from the crypt: genome mining from fungarium specimens improves resolution of the mushroom tree of life. Biological Journal of the Linnean Society. 117:11–32.

Dentinger BTM, Suz LM. 2014. What's for dinner? Undescribed species of porcini in a commercial packet. PeerJ. 2:e570.

Drehmel D, James T, Vilgalys R. 2008. Molecular phylogeny and biodiversity of the boletes. Fungi. 1:17—23.

Elliott TF, Jusino MA, Trappe JM, Lepp H, Ballard GA, Bruhl JJ, Verns K. 2019. A global review of the ecological significance of symbiotic associations between birds and fungi. Fungal Diversity. 98:161—194.

673 Feng F, Xu J, Wu G, Zeng NK, Li YC, Tolgor B, Kost GW, Yang ZL. 2012. DNA
674 sequence analyses reveal abundant diversity, endemism and evidence for Asian origin
675 of the porcini mushrooms. PLOS ONE. 7:e37567.
676
677 Feng YJ, Blackburn DC, Liang D, Hillis DM, Wake DB, Zhang P. 2017.
678 Phylogenomics reveals rapid, simultaneous diversification of three major clades of
679 Gondwanan frogs at the Cretaceous–Paleogene boundary. Proceedings of the National
680 Academy of Sciences. 114:E5864—E5870.
681
682 Fulgenzi TD, Halling RE, Henkel TW. 2010. *Fistulinella cinereoalba* sp. nov. and new
683 distribution records for *Austroboletus* from Guyana. Mycologia. 102:224–232.
684
685 Fulgenzi TD, Henkel TW, Halling RE. 2007. *Tylopilus orsonianus* sp. nov. and
686 *Tylopilus eximius* from Guyana. Mycologia. 99:622–627.
687
688 Fulgenzi TD., Mayor JR, Henkel TW, Halling RE. 2008. New species of *Boletellus*
689 from Guyana. Mycologia. 100:490–495.
690
691 Futuyma DJ. 1998. Evolutionary Biology. Quarterly Review of Biology. 73.
692
693 Galante TE, Horton TR, Swaney DP. 2011. 95% of basidiospores fall within 1 m of the
694 cap: a field-and modeling-based study. Mycologia. 103:1175–1183.
695
696 Geml , Timling I, Robinson CH, Lennon N, Nusbaum CH, Brochmann C, Noordeloos
697 ME, Taylor DL. 2012. An arctic community of symbiotic fungi assembled by long-

698 distance dispersers: phylogenetic diversity of ectomycorrhizal basidiomycetes in
699 Svalbard based on soil and sporocarp DNA. Journal of Biogeography. 39:74—88.
700
701 Golan JJ and Pringle A. 2017. Long-distance dispersal of fungi. Microbiology
702 Spectrum. 5:5—4.
703
704 Grigoriev IV, Nikitin R, Haridas S, Kuo A, Ohm R, Otillar R, Riley R, Salamov A,
705 Zhao X, Korzeniewski F, Smirnova T, Nordberg H, Dubchak I, Shabalov I. 2013.
706 MycoCosm portal: gearing up for 1000 fungal genomes. Nucleic Acids Research.
707 42:699–704
708
709 Grubisha LC, Trappe JM, Molina R, Spatafora JW. 2001. Biology of the
710 ectomycorrhizal genus *Rhizopogon*. V. Phylogenetic relationships in the Boletales
711 inferred from LSU rDNA sequences. Mycologia. 93:82–89.
712
713 Hackel J, Henkel TW, Moreau PA, De Crop E, Verbeken A, Sa M, Buyck B, Neves
714 MA, Vasco-Palacios A, Wartchow F, Schimann H, Carriconde F, Garnica S,
715 Courtecuisse R, Gardes M, Manzi S, Louisanna E, Roy M. 2022. Biogeographic history
716 of a large of ectomycorrhizal fungi, the Russulaceae, in the Neotropics and adjacent
717 regions. New Phytologist. 236:698—713.
718
719 Halling RE. 1996. Boletaceae (Agaricales): Latitudinal biodiversity and biological
720 interactions in Costa Rica and Colombia. Revista de Biología Tropical. 44:111–114.
721

722 Halling RE, Desjardin DE, Fechner N, Arora D, Soytong K, Dentinger BTM. 2014.
723 New Porcini (Boletus sect. Boletus) from Australia and Thailand. Mycologia. 106:830–
724 834.
725
726 Halling RE, Fechner NA, Holmes G, Davoodian N. 2023. *Kagaria* (Boletaceae,
727 Boletoideae) gen. nov. in Australia: Neither a *Tylopilus* nor a *Porphyrellus*. Fungal
728 Systematics and Evolution. 12:31—45.
729
730 Halling RE, Fechner N, Nuhn M, Osmundson T, Soytong K, Arora D, Binder M,
731 Hibbett D. 2015. Evolutionary relationships of *Heimioporus* and *Boletellus* (Boletales),
732 with an emphasis on Australian taxa including new species and new combinations in
733 *Aureoboletus*, *Hemileccinum* and *Xerocomus*. Australian Systematic Botany. 28:1–22.
734
735 Halling RE, Osmundson TW, Neves MA. 2006. *Austroboletus mutabilis* from northern
736 Queensland. Muelleria. 24:31–36.
737
738 Halling RE, Nuhn M, Osmundson T, Fechner N, Trappe JM, Soytong K, Arora D,
739 Hibbett DS, Binder M. 2012. Affinities of the *Boletus chromapes* group to *Royoungia*
740 and the description of two new genera, *Harrya* and *Australopilus*. Australian Systematic
741 Botany. 25:418–431.
742
743 Halling RE, Osmundson TE, Neves MA. 2008. Pacific boletes: implications for
744 biogeographic relationships. Mycological Research. 112:437–447.
745

746 He MQ, Zhao RL, Hyde KD, Begerow D, Kemler M, Yurkov A, McKenzie EHC,
747 Raspé O, Kakishima M, Sánchez-Ramírez S, Vellinga EC, Halling RE, Papp V,
748 Zmitrovich IV, Buyck B, Ertz D, Wijayawardene NN, Cui BK, Schoutteten N, Liu XZ,
749 Li TH, Yao YJ, Zhu XY, Liu AQ, Li GJ, Zhang MZ, Ling ZL, Cao B, Antonín V,
750 Boekhout T, da Silva BDB, De Crop E, Decock C, Dima B, Dutta AK, Fell JW, Geml J,
751 Ghobad-Nejhad M, Giachini AJ, Gibertoni TB, Gorjón SP, Haelewaters D, He SH,
752 Hodkinson BP, Horak E, Hoshino T, Justo A, Lim YW, Menolli N, Mešić A,
753 Moncalvo JM, Mueller GM, Nagy LG, Nilsson RH, Noordeloos M, Nuytinck J, Orihara
754 T, Ratchadawan C, Rajchenberg M, Silva-Filho AGS, Sulzbacher MA, Tkalčec Z,
755 Valenzuela R, Verbeken A, Vizzini A, Wartchow F, Wei TZ, Weiß M, Zhao CL, Kirk
756 PM. 2020. Notes, outline and divergence times of Basidiomycota. Fungal Diversity.
757 99:105—367.
758
759 Han LH, Feng B, Wu G, Halling RE, Buyck B, Yorou NS, Ebika STN, Yang ZL. 2018.
760 African origin and global distribution patterns: Evidence inferred from phylogenetic and
761 biogeographical analyses of ectomycorrhizal fungal genus *Strobilomyces*. Journal of
762 Biogeography. 45:201—212.
763
764 Hay WW and Floegel S. 2012. New thoughts about the Cretaceous climate and oceans.
765 Earth-Science Reviews. 115:262—272.
766
767 Heinemann P. 1951. Champignons recoltes au Congo belge par Madame M. Goossens-
768 Fontana I. Boletineae. Bulletin du Jardin botanique de l'État a Bruxelles. 21:223–346.
769

770 Henkel TW, Aime MC, Chin M, Miller SL, Vigalys R, Smith ME. 2012.
771 Ectomycorrhizal fungal sporocarp diversity and discovery of new taxa in *Dicymbe*
772 monodominant forests of the Guiana Shield. Biodiversity and Conservation. 21:2195—
773 2220.
774
775 Henkel TW, Obase K, Husbands D, Uehling JK, Bonito G, Aime MC, Smith ME. 2016.
776 New Boletaceae taxa from Guyana: *Binderoboletus* segoi gen. and sp. nov.,
777 *Guyanaporus albipodus* gen. and sp. nov., *Singerocomus rubriflavus* gen. and sp. nov.,
778 and a new combination for *Xerocomus inundabilis*. Mycologia. 108:157–173.
779
780 Hibbett DS. 2004. Trends in morphological evolution in Homobasidiomycetes inferred
781 using maximum likelihood: a comparison of binary and multistate approaches.
782 Systematic Biology. 53:889–903.
783
784 Hibbett DS, Pine EM, Langer E, Langer G, Donoghue MJ. 1997. Evolution of gilled
785 mushrooms and puffballs inferred from ribosomal DNA sequences. Proceedings of the
786 National Academy of Sciences. 94:12002–12006.
787
788 Hoang DT, Chernomor O, von Haeseler A, Minh BQ, Vinh LS. 2018. UFBoot2:
789 Improving the ultrafast bootstrap approximation. Molecular Biology and Evolution.
790 35:518–522.
791
792 Horak E. 1977. New and rare boletes from Chile, *Nothofagus chilenos*, Gas*troboletus*
793 *valdivians*, *Boletus loyita*, *Boletus putidus*. Boletín de la Sociedad Argentina de
794 Botánica.

795

796 Hosaka K, Castellano MA, Spatafora JW. 2008. Biogeography of Hysterangiales
797 (Phallomycetidae, Basidiomycota. Mycological Research. Phylogeography and
798 Biogeography of Fungi. 112:448–462.

799

800 Hu X, Garxanti E, Wang J, Huang W, An W, Webb A. 2016. The timing of India-Asia
801 collision onset–facts, theories, controversies. Earth Science Reviews. 160:264—299.

802

803 Husbands DR, Henkel TW, Bonito G, Vilgalys R, Smith ME. 2013. New species of
804 *Xerocomus* (Boletales) from the Guiana Shield, with notes on their mycorrhizal status
805 and fruiting occurrence. Mycologia. 105:422–435.

806

807 Jokat W, Boebel T, Konig M, Meyer U. 2003. Timing and geometry of early Gondwana
808 breakup. Journal of Geophysical Research: Solid Earth. 108:2156—2202.

809

810 Kalyaanamoorthy S, Minh BQ, Wong TKF, von Haeseler A, Jermiin LS. 2017.
811 ModelFinder: fast model selection for accurate phylogenetic estimates. Nature Methods.
812 14:587–589.

813

814 Katoh K, Rozewicki J, Yamada KD. 2017. MAFFT online service: multiple sequence
815 alignment, interactive sequence choice and visualization. Briefings in Bioinformatics.
816 20:1160—1166.

817

818 Kennedy PG, Matheny PB, Ryberg KM, Henkel TW, Uehling JK, Smith ME. 2012.
819 Scaling up: examining the macroecology of ectomycorrhizal fungi. Molecular Ecology.
820 21:4151–4154.
821
822 Kohler A, Kuo A, Naga LG, Morin E, Berry KW, Buscot F, Canback B, Choi C,
823 Cichocki N, Clum A, Colpaert J, Copeland A, Costa MD, Dore J, Floudas D, Gay G,
824 Girlanda M, Henrissat B, Herrmann S, Hess J, Hogberg N, Johansson T, Khouja HR,
825 LaButti K, Lahrmann U, Levasseur A, Lindquist EA, Lipzen A, Marmeisse R, Martino
826 E, Murat C, Ngan CY, Nehls U, Plett JM, Pringle A, Ohm RA, Perotto S, Peter M,
827 Riley R, Rineau F, Ruytinx J, Salamov A, Shah F, Sun H, Tarkka M, Tritt A, Veneault-
828 Fourrey C, Zuccaro A, Mycorrhizal Genomics Initiative Consortium, Tunlid A,
829 Grigoriev IG, Hibbett DS, Martin F. 2015. Convergent losses of decay mechanisms and
830 rapid turnover of symbiosis genes in mycorrhizal mutualists. Nature Genetics. 47:410–
831 415.
832
833 Landis MJ, Matzke NJ, Moore BR, Huelsenbeck JP. 2013. Bayesian analysis of
834 biogeography when the number of areas is large. Systematic Biology. 62:789–804.
835
836 Liimatainen K, Kim JT, Pokorny L, Kirk PM, Dentinger BTM, Niskanen T. 2022.
837 Taming the beast: a revised classification of Cortinariaceae based on genomic data.
838 Fungal Diversity. 112:89–170.
839
840 Liu Y, Xu X, Dimitrov D, Pellissier L, Borregaard MK, Shrestha N, Su X, Luo A,
841 Zimmermann NE, Rahbek C, Wang Z. 2023. An updated floristic map of the world.
842 Nature Communications. 14:2990.

Magnago AC, Neves MA, da Silveira RMB. 2017. *Fistulinella ruschii*, sp. nov., and a new record of *Fistulinella campinaranae var. scrobiculata* for the Atlantic Forest, Brazil. Mycologia. 109:1003—1013.

Matheny PB, Aime MC, Bougher NL, Buyck B, Desjardin DE, Horak E, Kropp BR, Lodge DJ, Soytong K, Trappe JM, Hibbett DS. 2009. Out of the Palaeotropics? Historical biogeography and diversification of the cosmopolitan ectomycorrhizal mushroom family Inocybaceae. Journal of Biogeography. 36:577–592.

Meade A and Pagel M. 2022. Ancestral state reconstruction using BayesTraits. Environmental Microbial Evolution: Methods and Protocols. New York, NY: Springer US. 255-266.

Minh BQ, Schmidt HA, Chernomor O, Schrempf D, Woodhams MD, von Haeseler A, Lanfear R. 2020. IQ-TREE 2: new models and efficient methods for phylogenetic inference in the genomic era. Molecular Biology and Evolution. 37:1530–1534.

Miyauchi S, Kiss E, Kuo A, Drula E, Kohler A, Sánchez-García M, Morin E, Andreopoulos B, Barry KW, Bonito G, Buée M, Carver A, Chen C, Cichocki N, Clum A, Culley D, Crous PW, Fauchery L, Girlanda M, Hayes RD, Kéri Z, LaButti K, Lipzen A, Lombard V, Magnuson J, Maillard F, Murat C, Nolan M, Ohm RA, Pangilinan J, Pereira MF, Perotto S, Peter M, Pfister S, Riley R, Sitrit Y, Stielow JB, Szöllősi G, Žifčáková L, Štursová M, Spatafora JW, Tedersoo L, Vaario LM, Yamada A, Yan M, Wang P, Xu J, Bruns T, Baldrian P, Vilgalys R, Dunand C, Henrissa Bt, Grigoriev IV,

868 Hibbett D, Nagy LG, Martin FM. 2020. Large-scale genome sequencing of mycorrhizal
869 fungi provides insights into the early evolution of symbiotic traits. Nature
870 Communications. 11:5125.
871
872 Murrill WA. 1909. The Boletaceae of North America—I. Mycologia. 1:4–18.
873
874 Nei M, Kumar S. 2000. Molecular evolution and phylogenetics. Oxford, New York:
875 Oxford University Press; p. 352.
876
877 Neves MA, Halling RE. 2010. Study on species of *Phylloporus* I: Neotropics and North
878 America. Mycologia. 102:923–943.
879
880 Norton IO, Sclater, JG. 1979. A model for the evolution of the Indian Ocean and the
881 breakup of Gondwanaland. Journal of Geophysical Research. 84:6803–6830.
882
883 Nuhn ME, Binder M, Taylor AFS, Halling RE, Hibbett DS. 2013. Phylogenetic
884 overview of the Boletineae. Fungal Biology. 117:479–511.
885
886 Peay KG, Kennedy PG, Davies SJ, Tan S, Bruns TD. 2010. Potential link between plant
887 and fungal distributions in a dipterocarp rainforest: community and phylogenetic
888 structure of tropical ectomycorrhizal fungi across a plant and soil ecotone. New
889 Phytologist. 185:529—542
890

891 Peay KG, Schubert MG, Nguyen NH, Bruns TD. 2012. Measuring ectomycorrhizal
892 fungal dispersal: macroecological patterns driven by microscopic propagules. Molecular
893 Ecology. 21:4122—4136.
894
895 Pegler DN, Young TWK. 1981. A natural arrangement of the Boletales, with reference
896 to spore morphology. Transactions of the British Mycological Society. 76:103–146.
897
898 Peintner U, Bougher NL, Castellano MA, Moncalvo JM, Moser MM, Trappe JM,
899 Vigalys R. 2001. Multiple origins of sequestrate fungi related to *Cortinarius*
900 (Cortinariaceae). American Journal of Botany. 88:2168-2179.
901
902 Raidl S. 1997. Studien zur ontogenese rhizomorphen von ektomykorrhiza. Bibliotheca
903 Mycologica 169:1–184.
904
905 Rambaut A, Drummond AJ, Xie D, Baele G, Suchard MA. 2018. Posterior
906 summarization in bayesian phylogenetics ssing Tracer 1.7. Systematic Biology. 67:901–
907 904.
908
909 Ree RH, Moore BR, Webb CO, Donoghue MJ. 2005. A likelihood framework for
910 inferring the evolution of geographic range on phylogenetic trees. Evolution. 59:2299–
911 2311.
912
913 Reguero MA, Goin FJ. 2021. Paleogeography and biogeography of the Gondwanan
914 final breakup and its terrestrial vertebrates: New insights from southern South America

915 and the “double Noah's Ark” Antarctic Peninsula. Journal of South American Earth
916 Sciences. 108:103358.
917
918 Rivas-Ferreiro M, Skarha SM, Rakotonasolo F, Suz LM, Dentinger BTM. 2023. DNA-
919 based fungal diversity in Madagascar and arrival of the ectomycorrhizal fungi to the
920 island. Biotropica. 55:954-968.
921
922 Ronquist F. 1994. Ancestral areas and parsimony. Systematic Biology. 43:0267– 274.
923
924 Ryberg M and Matheny PB. 2011. Dealing with incomplete taxon sampling and
925 diversification of a large clade of mushroom-forming Fungi. Evolution. 65:1862–1878.
926
927 Sánchez-García M, Ryberg M, Khan FK, Hibbett DS. 2020. Fruiting body form, not
928 nutritional mode, is the major driver of diversification in mushroom-forming fungi.
929 Proceedings of the National Academy of Sciences. 117:32528–32534.
930
931 Sánchez-Ramírez S, Ryberg M, Khan FK, Varga T, Nagy LG, Hibbett DS. 2015. High
932 speciation rate at temperate latitudes explains unusual diversity gradients in a clade of
933 ectomycorrhizal fungi. Evolution. 69:2196–2209.
934
935 Sato H, Tanabe AS, Toju H. 2017. Host shifts enhance diversification of
936 ectomycorrhizal fungi: diversification rate analysis of the ectomycorrhizal fungal genera
937 *Strobilomyces* and *Afroboletus* with an 80-gene phylogeny. New Phytologist. 214: 443–
938 454.
939

940 Sato H, Toju H. 2019. Timing of evolutionary innovation: scenarios of evolutionary
941 diversification in a species-rich fungal clade, Boletales. New Phytologist. 222:1924–
942 1935.
943
944 Schluter D. 2000. Ecological character displacement in adaptive radiation. The
945 American Naturalist. 156:4–16.
946
947 Simões M, Breitkreuz L, Alvarado M, Baca S, Cooper JC, Heins L, Herzog K,
948 Lieberman BS. 2016. The evolving theory of evolutionary radiations. Trends in Ecology
949 & Evolution, 31:27–34.
950
951 Singer R. 1945a. The Boletineae of Florida with notes on extralimital species I. The
952 Strobilomycetaceae. Farlowia. 2:97–141.
953
954 Singer R. 1945b. The Boletineae of Florida with notes on extralimital species. II. The
955 Boletaceae. Farlowia. 2:223–303
956
957 Singer R. 1947. The Boletoideae of Florida with notes on extralimital Species III. The
958 American Midland Naturalist. 37:1–135.
959
960 Singer R and Digilio AP. 1951. Pródromo de la flora agaricina argentina. Lilloa. 5–461.
961
962 Sitta N, Floriani M. 2008. Nationalization and globalization trends in the wild
963 mushroom commerce of Italy with emphasis on porcini (*Boletus edulis* and allied
964 species. Economic Botany. 62:307.

965

966 Smith MR. 2020. Information theoretic generalized Robinson–Foulds metrics for
967 comparing phylogenetic trees. Bioinformatics. 36:5007–5013.

968

969 Smith MR. 2022. Robust analysis of phylogenetic tree space. Systematic Biology.
970 71:1255–1270.

971

972 Smith SA, Brown JW, Walker JF. 2018. So many genes, so little time: A practical
973 approach to divergence-time estimation in the genomic era. PLOS ONE. 13:e0197433.

974

975 Soulebeau A, Aubriot X, Gaudeul M, Rougan G, Hennequin S, Haevermans T,
976 Dubuisson JY, Jabbour F. 2015. The hypothesis of adaptive radiation in evolutionary
977 biology: hard facts about a hazy concept. Organisms Diversity & Evolution. 15:747–
978 761.

979

980 Stecher G, Tamura K, Kumar S. 2020. Molecular evolutionary genetics analysis
981 (MEGA) for macOS. Molecular Biology and Evolution. 37:1237–1239.

982

983 Storey B. 1995. The role of mantle plumes in continental breakup: case histories from
984 Gondwanaland. Nature. 377:301–308.

985

986 Šutara J. 2005. Central European genera of the Boletaceae and Suillaceae, with notes on
987 their anatomical characters. Czech Mycology. 57:1–50.

988

989 Šutara J. 2014. Anatomical structure of pores in European species of genera *Boletus*
990 s.str. and *Butyriboletus* (Boletaceae). Czech Mycology. 66:157–170.
991
992 Tamura K, Battistuzzi FU, Billing Ross P, Murillo O, Filipski A, Kumar S. Estimating
993 divergence times in large molecular phylogenies. Proceedings of the National Academy
994 of Sciences. 109:19333–19338.
995
996 Tamura K, Stecher G, Kumar S. 2021. MEGA11: molecular evolutionary genetics
997 analysis Version 11. Molecular Biology and Evolution. 38:3022–3027.
998
999 Tamura K, Tao Q, Kumar S. 2018. Theoretical foundation of the RelTime method for
1000 estimating divergence times from variable evolutionary rates. Molecular Biology and
1001 Evolution. 35:1770–1782.
1002
1003 Tao Q, Tamura K, Kumar S. 2020. Efficient methods for dating evolutionary
1004 divergences. Pp. 197– 219 in Ho SYW (Ed.) The molecular evolutionary clock: theory
1005 and practice. Cham, Switzerland: Springer Nature Switzerland AG.
1006
1007 Thiel M and Gutow L. 2005. The ecology of rafting in the marine environment. II. The
1008 rafting organisms and community. Oceanography and Marine Biology. 43:279—418.
1009
1010 Thiers HD. 1984. The secotioid syndrome. Mycologia, 76:1–8.
1011

1012 Tremble K, Hoffman JI, Dentinger BTM. 2022. Contrasting continental patterns of
1013 adaptive population divergence in the holarctic ectomycorrhizal fungus *Boletus edulis*.
1014 New Phytologist. 237:295—309.
1015
1016 Tremble K, Suz LM, Dentinger BTM. 2020. Lost in translation: population genomics
1017 and long-read sequencing reveals relaxation of concerted evolution of the ribosomal
1018 DNA cistron. Molecular Phylogenetics and Evolution. 148:106804.
1019
1020 Tremble K, Halling RE, Henkel TW, Moncalvo JM, Dentinger BTM. 2023.
1021 Nomenclatural novelties. Index Fungorum no. 555.
1022 https://www.indexfungorum.org/Publications/Index%20Fungorum%20no.555.pdf
1023
1024 Varga T, Krizsán K, Földi C, Dima B, Sánchez-García M, Sánchez-Ramírez S, Szöllősi
1025 GJ, Szarkándi JG, Papp V, Albert L, Andreopoulos W, Angelini C, Antonín V, Barry
1026 KW, Bougher NL, Buchanan P, Buyck B, Bense V, Catcheside P, Chovatia M, Cooper
1027 J, Dämon W, Desjardin D, Finy P, Geml J, Haridas S, Hughes K, Justo A, Karasiński D,
1028 Kautmanova I, Kiss B, Kocsubé S, Kotiranta H, LaButti KM, Lechner BE, Liimatainen
1029 K, Lipzen A, Lukács Z, Mihaltcheva S, Morgado LN, Niskanen T, Noordeloos ME,
1030 Ohm RA, Ortiz-Santana B, Ovrebo C, Rácz N, Riley R, Savchenko A, Shiryaev A,
1031 Soop K, Spirin V, Szebenyi C, Tomšovský M, Tulloss RE, Uehling J, Grigoriev IV,
1032 Vágvölgyi C, PappT, Martin FM, Miettinen O, Hibbett DS, Nagy LG. 2019.
1033 Megaphylogeny resolves global patterns of mushroom evolution. Nature Ecology &
1034 Evolution. 3:668–678.
1035

1036 Vellinga EC, Kuyper TW, Ammirati J, Desjardin DE, Halling RE, Justo A, Laessoe T,
1037 Lebel T, Lodge DJ, Matheny PB, Methven AS, Moreau PA, Mueller GM, Noordeloos
1038 ME, Nuytinck J, Ovrebo CL, Verbeken A. 2015. Six simple guidelines for introducing
1039 new genera of fungi. IMA Fungus. 6:A65–A68.
1040
1041 Wilf P, Nixon KC, Gandolfo MA, Cuneo NR. 2019. Eocene Fagaceae from Patagonia
1042 and Gondwanan legacy in Asian rainforests. Science. 364:5139.
1043
1044 Wilson AW, Binder M, Hibbett DS. 2011. Effects of gasteroid fruiting body
1045 morphology on diversification rates in three independent clades of fungi estimated using
1046 binary state speciation and extinction analysis. Evolution. 65:1305—1322.
1047
1048 Wu G, Feng B, Xu J, Zhu XT, Li YC, Zeng NK, Hosen MI, Yang ZL. 2014. Molecular
1049 phylogenetic analyses redefine seven major clades and reveal 22 new generic clades in
1050 the fungal family Boletaceae. Fungal Diversity. 69:93–115.
1051
1052 Wu G, Miyauchi S, Morin E, Kuo A, Drula E, Varga T, Kohler A, Feng B, Cao Y,
1053 Lipzen A, Daum C, Hundley H, Pangilinan J, Johnson J, Barry K, LaButti K, Ng V,
1054 Ahrendt S, Min B, Choi IG, Park H, Plett JM, Magnuson J, Spatafora JW, Nagy LG,
1055 Henrissat B, Grigoriev IV, Yang ZL, Xu J, Martin FM. 2022. Evolutionary innovations
1056 through gain and loss of genes in the ectomycorrhizal Boletales. New Phytologist.
1057 233:1383–1400.

1058 **LEGENDS**

1059 **Table 1.** Morphological transition rates estimated with Bayestraits.

Figure 1. Selected Boletaceae collections from two of the most species-rich regions that were newly sequenced in this study. A) *Boletus cervinococcineus*, Singapore (BD616); B) *Heimioporus punctisporus*, Sarawak (BAKO2); C) unidenti- fied Boletaceae, Vietnam (CTN-08-0007); D) unidentified Boletaceae (CTN-08-0029); E) *Spongiforma* sp., Sarawak (BTNG10); F) *Leccinum* sp., Sarawak (SWK246); G) *Crocinoboletus laetissimus*, Sarawak (SWK335); H) unidentified Boletaceae sp., Viet- nam (DLT-08-0127); I) *Boletellus* sp., Sarawak (SWK356); J) unidentified Boletaceae, Vietnam (CTN-08-0051); K) *Tylopilus* sp., Cameroon (BD655); L) *Xerocomus* sp. 9. Cameroon (BD773); M) *Fistulinella staudtii*, Cameroon (BD848); N) *Boletellus* sp., Cameroon (BD714); O) *Phylloporus cf. tubipes*, Cameroon (BD719); P) *Tylopilus* sp. 8, Cameroon (BD816); Q) *Xerocomus* sp. 8, Cameroon (BD695); R) *Boletus alliaceus*, Cameroon (BD697); S) *Tubosaeta brunneosetosa*, Cameroon (BD686); T) *Tylopilus* sp., Cameroon (BD716). Not to scale.

Figure 2. Time-calibrated phylogeny of Boletaceae using 1764 BUSCO genes. Topology is a summary coalescent of individual best ML gene trees using astral-hybrid. Numbers on branches are quartet probabilities. Branch lengths were converted to time using the top 100 best gene trees estimated using SortaDate in RelTime. Inset a) map of specimen origins with numbers of specimens from each geographic area. Inset b) lineages-through-time plot calculated with the “ltt.plot” function in the R pack- age “ape.” The dashed line represents a constant birth-death rate. The shaded box indicates a period of significant divergent increase from a constant birth-death rate indicative of a rapid radiation.

Figure 3. Biogeographic reconstruction using BioGeoBEARS. Left-hand tree depicts 4-state coding scheme (light blue=Neotropical, blue=Paleotropical, yellow=North Temperate, red=South Temperate) and right-hand tree depicts floristic region coding

scheme (pink=Chilean-Patagonian, green=Indo-Malesian, blue=African, yellow=Holarctic, red=Novo-Zealandic, light blue=Neotropical, orange=Australian). Pie charts indicate the proportional likelihood of each state at a node. Red and black boxes indicate Phase I and Phase II Gondwanan diversification events, respectively.

Figure 4. Dispersal events and rates inferred from BioGeoBEARS. Top: Map depicting phytogeographic zones that are colored and labeled on the map. Map was ren- dered using the 'imago' R code (https://github.com/hrbrmstr/imago) to reproduce the AuthaGraph world map projection (http://www.authagraph.com/top/?lang=en). Curved arrows indicate inferred directional dispersal events and are colored by rate values following the table (Bottom). The stroke weight of the arrows has been scaled to percent of the maximum rate value following the values in the table. Bottom: Table of dispersal rates inferred under a DIVAlike+j model in BioGeoBEARS. Source regions are at left and destination regions are along the top. Values are colored along a scale from cool to warm (red being maximum).

Figure 5. Distribution of likelihood frequencies of morphological traits. A-C) Illustrations of coded traits and inferred transition rates. Arrows indicate direction of transition with stroke weights scaled to maximum rate value. D-I) Frequency distributions of state probabilities for six trait codings. Traits and codes are labeled on the x-axis.

*Corresponding author: Email: keaton.tremble@gmail.com. Current address: Department of Biology, Duke University, Durham, North Carolina 27708.

Trait	Transition	Mean rate	Median rate
Ballistospory			
	Yes to No	1.2303	1.0565
	No to Yes	39.8088	35.7478
Spore Ornamentation			
	Smooth to Not Smooth	0.7747	0.7498
	Not Smooth to Smooth	1.741	1.464
Stipe			
	Absent to Present	33.685	27.67
	Present to Absent	0.8415	0.6788
Sporocarp Habit			
	Secoitiod to Pileate-stipitate	51.64	51.47
	Pileate-stipitate to Secoitiod	0.8178	0.7172
	Secoitiod to Gasteroid	53.44	53.90
	Gasteroid to Secoitiod	34.63	31.05
	Pileate-stipitate to Gasteroid	0.8393	0.6749
	Gasteroid to Pileate-stipitate	40.78	36.85
Hymenophore Bruising			
	None to Blue	1.3515	1.2632
	None to Black	0.6921	0.6921
	Blue to None	5.3730	5.3540
	Blue to Black	0.1732	0.1205
	Black to None	3.2329	2.7385
	Black to Blue	1.0294	0.7281
Hymenophore Anatomy			
	Straight to Cross	0.6398	0.6092
	Straight to Lamellete	0.2054	0.1715
	Cross to Straight	3.694	2.960
	Cross to Lamellate	2.4131	1.6755
	Lamellate to Straight	5.483	5.004
	Lamellate to Cross	1.858	1.275

Africa

Southeast Asia

*1764 BUSCO genes, ≥ 20% complete
*ASTER summary coalescent of best ML gene trees
*branch lengths converted to time in RelTime from 100 top-ranked trees using SortaDate

a

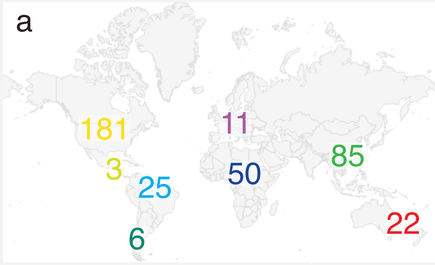

b

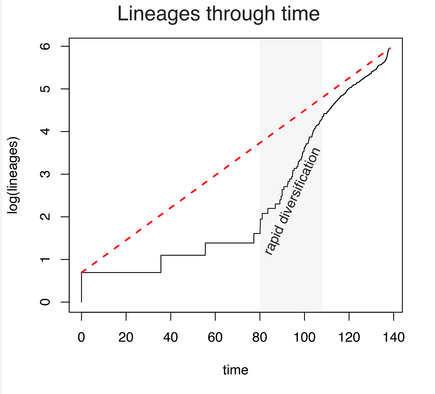

BOLETOIDEAE

Boletus s.s.
38 mya (95% CI: 14-90 mya)
30 mya
(95% CI: 11-78 mya)

SUILLELLOIDEAE

55 mya
(95% CI: 26-115 mya)

51 mya
(95% CI: 24-111 mya)

AUSTROBOLETOIDEAE

58 mya
(95% CI: 47-145 mya)

LECCINOIDEAE

61 mya
(95% CI: 31-122 mya)

XEROCOMOIDEAE

83 mya
(95% CI: 47-145 mya)

103 mya
(95% CI: 67-145 mya)

BOLETACEAE

138 mya
(95% CI: 50-150 mya)

57 mya
(95% CI: 28-117 mya)

ZANGIOIDEAE

PHYLLOBOLETELLOIDEAE

CHALCIPOROIDEAE

OUTGROUP

150
100
50
0
Time (millions of years)

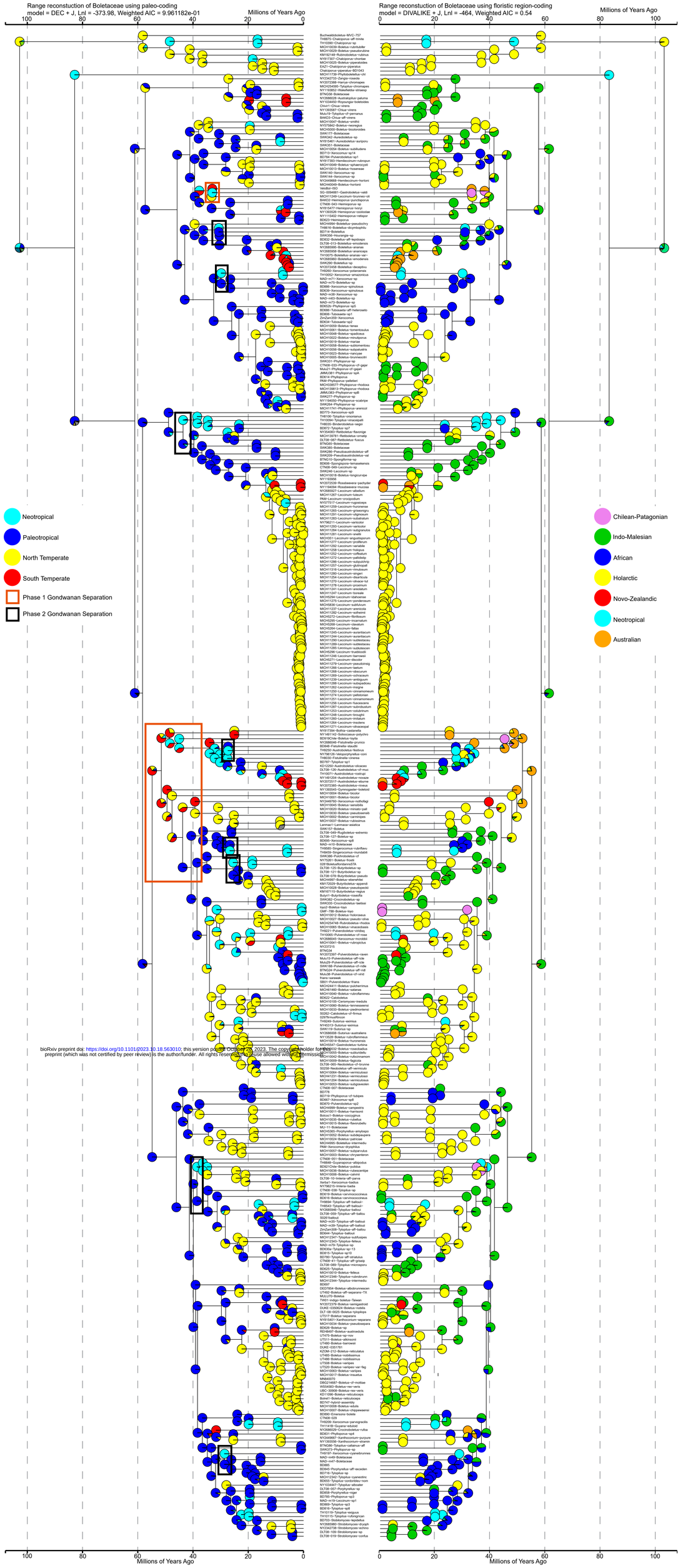

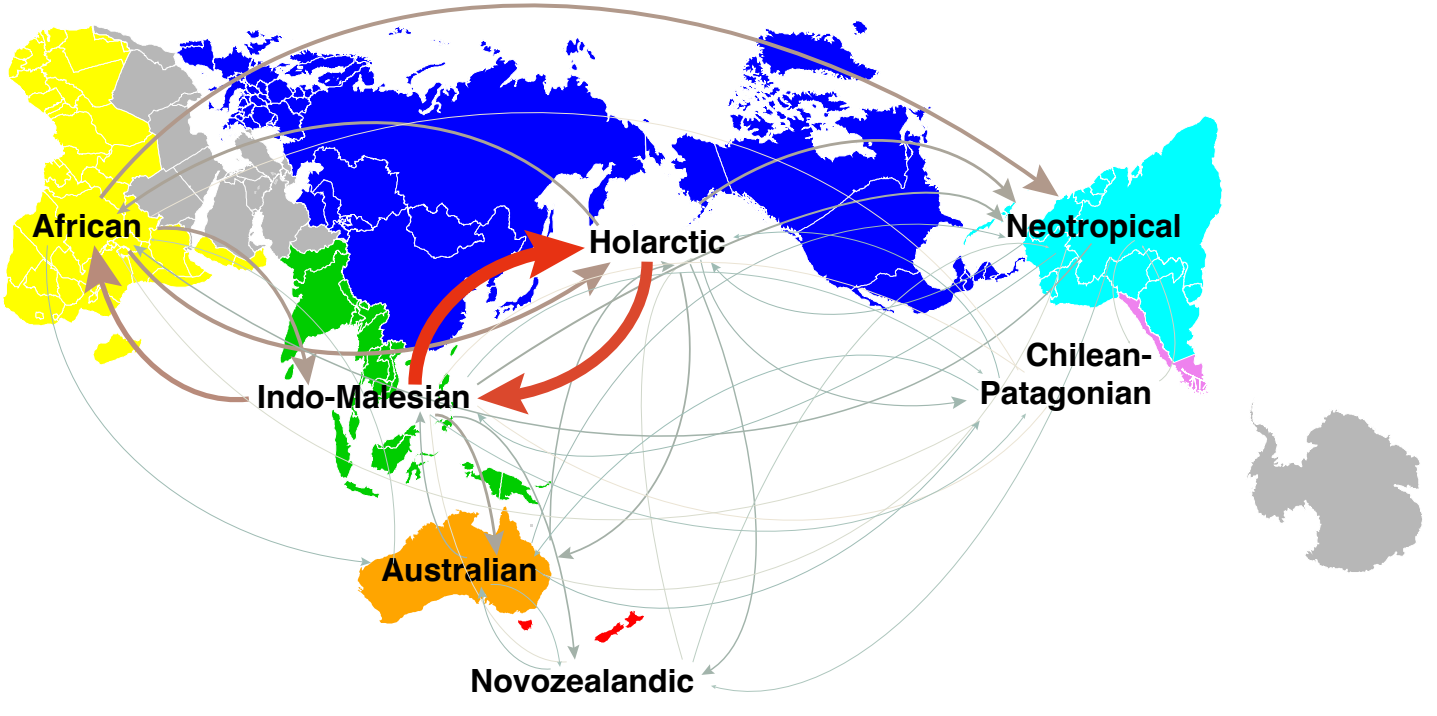

SOURCE	DESTINATION						
	Holarctic	Neotropical	Indo-Malesian	African	Australian	Novo-zealandic	Chilean-Patagonian
Holarctic	0	4.28	17.42	4.66	2.72	2.22	1.76
Neotropical	1.26	0	1.16	2.34	0.22	0.6	0.34
Indo-Malesian	20.52	3.12	0	8	4.32	2.54	0.64
African	6.46	6.1	5.56	0	1.24	0	0.2
Australian	2.38	1.34	2.16	0.5	0	0.66	1.06
Novozealandic	0.28	0.48	0.12	0	1.4	0	0
Chile-Patagonian	0.74	0.32	0.04	0.04	0.84	0	0

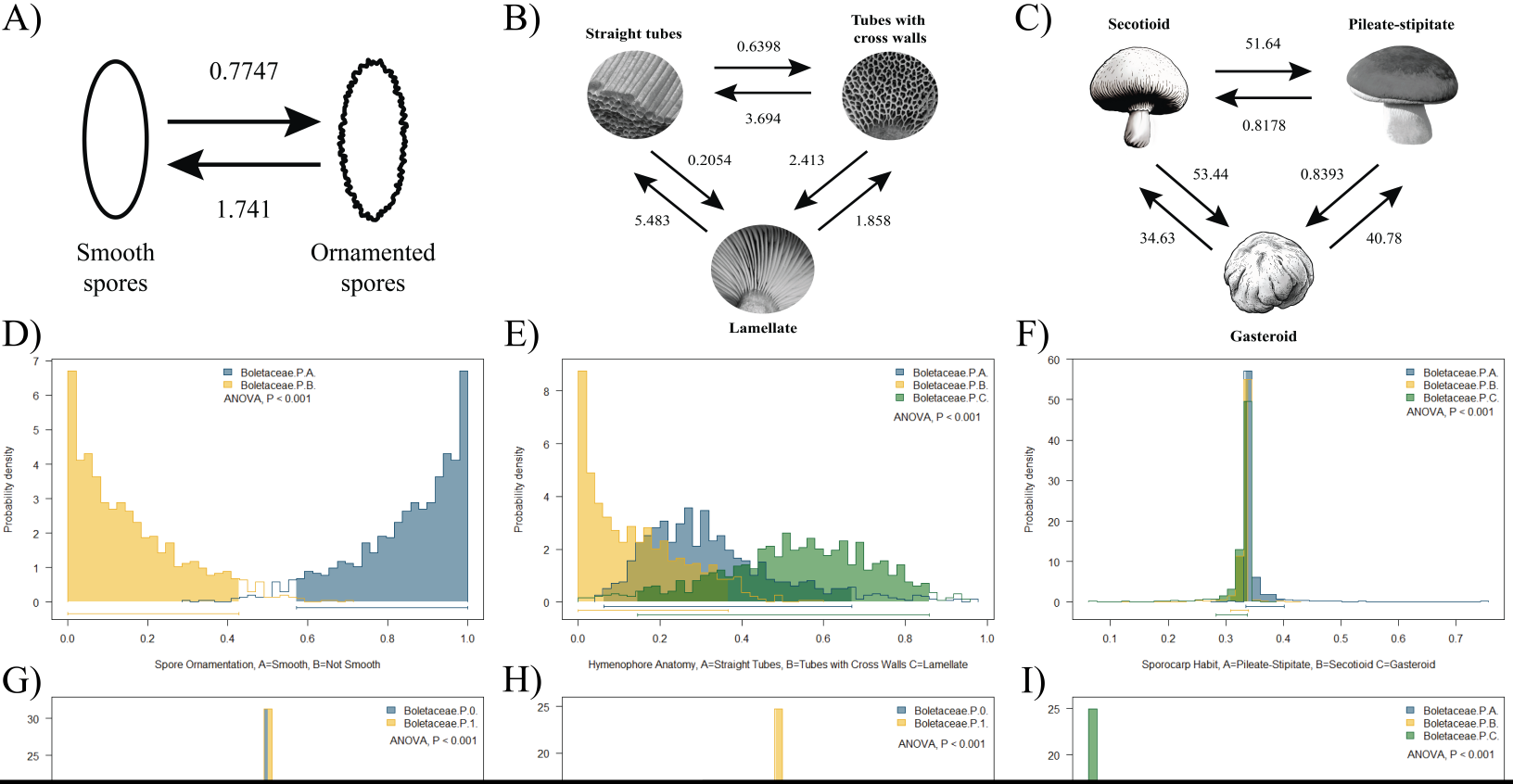
A)
0.7747
1.741
Smooth spores
Ornamented spores
B)
Straight tubes
Tubes with cross walls
0.6398
3.694
0.2054
5.483
2.413
1.858
Lamellate
C)
Secotioid
Pileate-stipitate
51.64
0.8178
53.44
34.63
0.8393
40.78
Gasteroid
D)
Boletaceae.P.A.
Boletaceae.P.B.
ANOVA, P < 0.001
Probability density
Spore Ornamentation, A=Smooth, B=Not Smooth
E)
Boletaceae.P.A.
Boletaceae.P.B.
Boletaceae.P.C.
ANOVA, P < 0.001
Probability density
Hymenophore Anatomy, A=Straight Tubes, B=Tubes with Cross Walls C=Lamellate
F)
Boletaceae.P.A.
Boletaceae.P.B.
Boletaceae.P.C.
ANOVA, P < 0.001
Probability density
Sporocarp Habit, A=Pileate-Stipitate, B=Secotioid C=Gasteroid
G)
Boletaceae.P.0.
Boletaceae.P.1.
ANOVA, P < 0.001
H)
Boletaceae.P.0.
Boletaceae.P.1.
ANOVA, P < 0.001
I)
Boletaceae.P.A.
Boletaceae.P.B.
Boletaceae.P.C.
ANOVA, P < 0.001